

Fracture Mechanics of Concrete Structures  
**Proceedings FRAMCOS-3**  
AEDIFICATIO Publishers, D-79104 Freiburg, Germany

## **FORMULATION OF SHEAR STRENGTH DESIGN FORMULA FOR REINFORCED CONCRETE BEAMS CONSIDERING SIZE EFFECT**

N. Shirai and K. Moriizumi,  
Department of Architecture, College of Science and Technology,  
Nihon University, Tokyo, Japan  
M. Tamura,  
Nishimatsu Construction, Tokyo, Japan

### **Abstract**

In the present study, three R/C beam specimens with the depth of 600, 900 and 1200mm were tested to clarify the size effect in large scale R/C beams. Furthermore, shear strength design equation is formulated on the basis of the multi-fractal scaling law modified with the fracture mechanics parameter and the current design formula. Finally, validity of the proposed formula is verified in comparison with the existing test data.

Key words: Size effect, reinforced concrete beam, shear strength design formula, multi-fractal scaling law, truss mechanism, arch mechanism.

### **1 Introduction**

The authors conducted the shear loading test on geometrically similar 9 R/C beam specimens and also analyzed these specimens by FEM with the

fictitious crack model in the previous study, Shirai et al. (1995). The major variables were as follows: the beam depth ( $D$ ) ranging from 150mm to 600mm, the spacing of shear reinforcement ( $S$ ), the shear span ratio ( $a/D$ ;  $a$ : shear span length), the maximum size of aggregate ( $d_a$ ) and the yield strength of shear reinforcement ( $f_{sy}$ ). The effect of variables on fracture mode, shear resistant mechanism and shear strength were rigorously investigated. The results indicated that the size effect on shear strength is caused even in the R/C beams with shear reinforcement. Furthermore, it was confirmed that variation of the fracture mode with the increase in  $D$ ; that is, transition of the shear resistant mechanism, would be a major source causing the size effect.

In recent years, a general size effect or scaling law for concrete has been proposed. The size effect law (SEL), Bazant (1984), and the multi-fractal scaling law (MFSL), Carpinteri et al. (1995), are the representative ones. SEL was derived by paying attention to the difference in the energy release per unit fracture extension, and MFSL was derived on the assumption of multi-fractality of damaged concrete microstructure. SEL and MFSL can be expressed by the following equations, respectively:

$$\sigma_N^{SEL} = Bf_t(1 + d/d_0)^{-1/2}, \quad \sigma_N^{MFSL} = Bf_t(1 + d_0/d)^\alpha \quad (1)$$

where,  $\sigma_N$  is the nominal strength;  $d$  is the characteristic size of members or structures;  $f_t$  is the tensile strength of concrete;  $B$  and  $d_0$  are the empirical constants; and  $\alpha$  is a fraction within  $0 < \alpha < 1$  and assumed to be  $\alpha = 1/2$  in the present study. Figure 1 shows the nominal shear strength ( $\tau_{AU}$ ) -  $D$  relation expressed by the logarithmic scale. The test results by the authors, Shirai et al. (1995), and the calculated values by SEL and MFSL are compared in the figure. Note that the empirical constants in SEL and MFSL were identified by applying the best-fit method to the test data. SEL indicates that  $\tau_{AU}$  gradually decreases with the increase in  $D$  value and finally approaches asymptotically to zero value. On the other hand, MFSL shows that the size effect disappears in the range with larger  $D$  values and  $\tau_{AU}$  approaches asymptotically to a certain constant value. In other words, both SEL and MFSL equally compare with the test results for  $D = 150$  to 600mm, but they give antithetical tendencies in the range of  $D$  values beyond 600mm. However, there has been no systematic experimental study on the size effect in large scale R/C beam specimens with  $D$  value exceeding 600mm so far, excepting the work by Walraven et al. (1994).

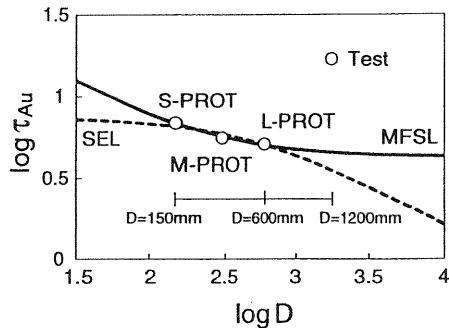


Fig.1 Size effect prediction

In order to investigate the size effect in large scale R/C beams, the shear loading test on geometrically similar 3 specimens, having  $D=600$ , 900 and 1,200mm, was conducted in the present study. The test results indicate that the size effect exists in the range of  $D$  value up to about 600 to 800mm, but beyond this the size effect disappears and  $\tau_{AU}$  approaches to a certain constant value with the increase in  $D$  value. Furthermore, it is shown that a major source causing the size effect may be due to transition of the shear resistant mechanism and particularly it is governed by the arch mechanism.

In the next place, the concept of “equivalent strength” is proposed on the basis of the fracture energy of concrete ( $G_F$ ), and then MFSL is modified using this equivalent strength. Furthermore, a rational shear strength design formula considering the size effect is formulated by applying the modified MFSL to the current design formula of the Architectural Institute of Japan (AIJ formula), AIJ (1990). Finally, validity of the proposed formula is verified through the comparison between the predicted values and the existing test results on 206 R/C beam specimens with  $D$  values ranging from 150 to 1,200mm.

## 2 Test program and results

### 2.1 Test program

In the present study, large scale geometrically similar specimens with different  $D$  values are so designed that the variables other than  $d_a$  and the compressive strength of concrete ( $f'_c$ ) are kept the same as those of the previous test; thus  $D$  is only the variable. Figure 2 shows the dimension and bar arrangement of typical specimen. The structural detail of specimens are listed in Table 1. The specimen referred to as “H” is the

present test series and "PROT" is the previous test ones. H-10 is the specimen with the same dimension as L-PROT, and H-15 and H-20 are 1.5 and 2.0 times the size of H-10 or L-PROT. Material properties of concrete and reinforcement are listed in Tables 2 and 3, respectively.

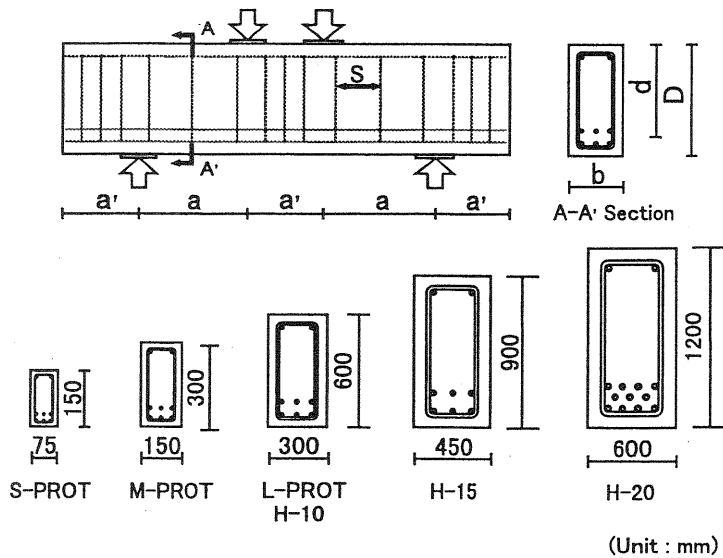


Fig.2 Detail of specimens

Table 1 Structural details of specimens

Specimen	Dimension(mm)					Shear reinforcement			Longitudinal Bar	
	b	D	d	a	a'	Type	S(mm)	Ps(%)	Type	Pt(%)
S-PROT	75	150	125	150	150	2-D3*	53		6-D6	2.06
M-PROT	150	300	249	300	200	2-D6	120	0.35	6-D13	2.04
L-PROT	300	600	498	600	200	2-D13	240		6-D25	
H-10	300	600	498	600	400	2-D13	240		6-D25	2.04
H-15	450	900	747	900	600	2-D19	360	0.35	6-D38	
H-20	600	1200	996	1200	800	2-D25	480		8-D38,3-D35	2.01

\* 2-D3 Indicates two deformed bars with nominal diameter of 3mm

Table 2. Material Properties of Concrete

Specimen	da (mm)	f <sub>c</sub> (MPa)	E <sub>c</sub> * (GPa)
S-PROT	13	28.5	26.0
M-PROT	13	29.0	24.6
L-PROT	13	29.1	23.7
H-10	20	22.9	26.7
H-15	20	23.1	26.9
H-20	20	25.2	27.1

\* Young's Modulus

Table 3. Material properties of reinforcement

Specimen	Type	f <sub>sy</sub> (MPa)	E <sub>s</sub> (GPa)
S-PROT	D3	370.1	173.6
M-PROT	D6	411.9	177.5
L-PROT	D13	376.3	193.2
H-10	D13	326.4	172.6
	D19	353.1	173.6
	D25	357.5	193.2
H-15	D25	418.7	188.3
	D35	442.9	181.4
	D38	439.0	186.3

\* Young's Modulus

The loading and measuring methods are shown in Fig. 3. The universal testing machines with the capacity of 1,961kN and 29,4200kN were adopted for loading in the "PROT" series and in the "H" series, respectively. Strains in longitudinal bars and shear reinforcement were measured using the strain gauges. Displacements were measured using the displacement transducers installed on front and rear sides of specimen. Vertical displacements at the loading points relative to the supporting points ( $\delta_v$ ) were measured. Note that extensions along the depth ( $\delta_s$ ) and along the member axis ( $\delta_h$ ) were also measured in the "H" series.

## 2.2 Test results and discussion

The nominal shear stress ( $\tau_A = Q/A_e$ ) shall be obtained by normalizing the applied shear force ( $Q$ ) by the effective area ( $A_e = b \cdot d_e$ ) as shown in Fig. 4. Where,  $d_e$  indicates the distance from the outermost fiber of tensile longitudinal bar to the outermost fiber of compressive concrete. The test results are summarized in Table 4. The flexural cracking strength ( ${}_b\tau_{cr}$ ), the shear cracking strength ( ${}_s\tau_{cr}$ ), the ultimate shear strength ( $\tau_u$ ), the vertical displacement at the peak load ( $\delta_{vu}/a$ ) and the fracture mode are listed in the table. Figure 5 shows the final cracking patterns. In the

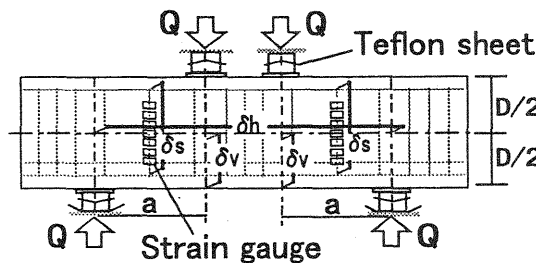


Fig.3 Loading and measuring method

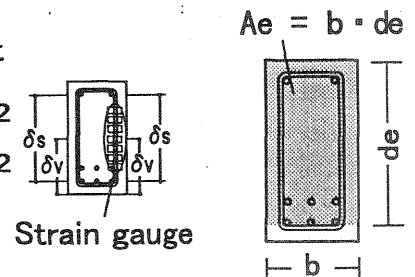


Fig.4 Effective area

Table 4 Summary of test results

Specimen	${}_b\tau_{cr}$ (MPa)	${}_s\tau_{cr}$ (MPa)	$\tau_u$ (MPa)	$\delta_{vu}/a$ (%)	Fracture mode
S-PROT	1.44	2.11	5.47	0.85	Shear compression
M-PROT	0.82	1.56	4.46	0.70	
L-PROT	0.48	1.50	4.09	0.61	
H-10	1.20	1.62	4.47	0.64	Shear sliding
H-15	0.79	1.41	4.69	0.72	
H-20	0.72	1.59	4.80	0.66	

specimens with larger  $D$  value, diagonal shear cracks penetrate the full depth of beam and sliding along crack surfaces leads to the final failure, which is referred to as the “sliding shear failure”. In the specimens with small  $D$  value, crushing of web concrete leads to the final failure, which is referred to as the “shear compression failure”.

Figures 6(a) and 6(b) compare  $\tau_A - \delta_v/a$  relations for the “PROT” and “H” series, respectively. The test result of L-da is also plotted in the figure. Note that L-da is the same specimen as L-PROT excepting  $d_a$ ; that is,  $d_a=13\text{mm}$  for L-PROT and  $d_a=25\text{mm}$  for L-da. For the “PROT” series,  $\tau_{AU}$  decreases with the increase in  $D$  value. Thus, the size effect can be observed. For the “H” series, on the other hand, the test results give almost similar  $\tau_{AU}$  irrespective of the increase in  $D$  value. However, softening behaviors after the peak load tend to become brittle with the increase in  $D$  value. Comparing  $\tau_{AU}$  for L-PROT ( $f'_c=29.1\text{MPa}$ ,

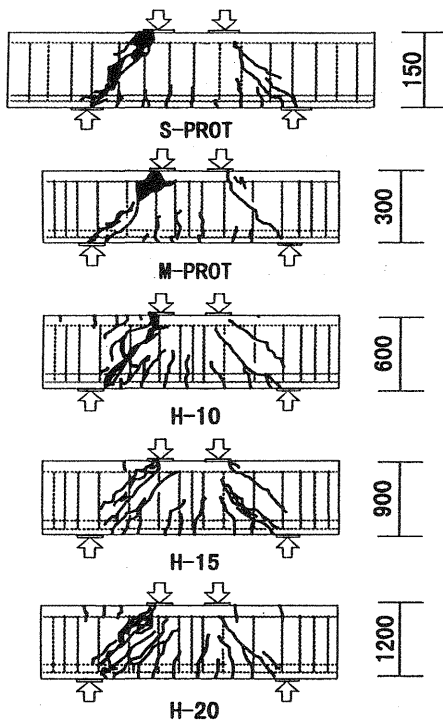
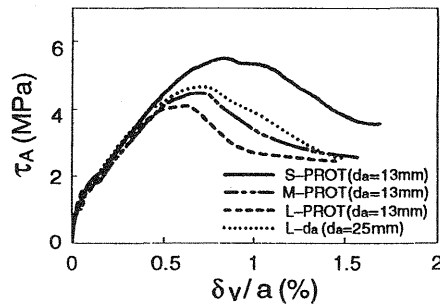
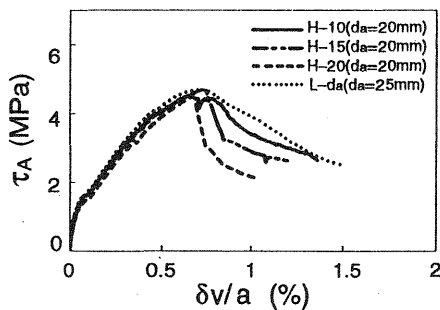


Fig.5 Observed crack patterns



(a) PROT series



(b) H series

Fig.6 Applied shear stress - vertical displacement relation

$d_a=13\text{mm}$ ), L-da ( $f'_c=29.3\text{MPa}$ ,  $d_a=25\text{mm}$ ) and H-10 ( $f'_c=22.9\text{MPa}$ ,  $d_a=20\text{mm}$ ),  $\tau_{AU}$  decreases in the order of L-da, H-10 and L-PROT; that is, L-da is the highest and L-PROT is the lowest. This fact suggests that the effect of  $d_a$  rather than  $f'_c$  on  $\tau_{AU}$  is significant. This may be explained by the following argument. Figure 7 shows variation in  $G_F$  against  $d_a$  and  $f'_c$  evaluated according to the CEB-FIP MODEL CODE 1990, CEB (1990). It is seen that the effect of  $d_a$  on  $G_F$  is significant rather than  $f'_c$ .  $f'_c$  for H-10 is lower than that for L-PROT, but  $d_a$  for H-10 is larger than that for L-PROT. Thus,  $G_F$  for H-10 becomes higher than that for L-PROT and this increase in  $G_F$  value leads to the increase in  $\tau_{AU}$ . This means that  $f'_c$  or  $f_i$  is not a suitable measure representing concrete property and a new measure based on  $G_F$  considering the effect of  $d_a$  must be established.

Figure 8 shows the plot of  $\tau_{AU}$  obtained from the test against  $D$  value. The test results by Walraven and the predicted values by SEL and MFSL are also plotted in the figure. Note that  $a/D=1.0$ ,  $p_i=0.3\%$  and  $b=250\text{mm}$  were fixed to be constant and only  $D$  value was varied in the test by Walraven. The size effect is clearly observed in these test results, and especially MFSL agrees fairly well with the tendency of test results. Note that  $\tau_{AU}$  is normalized by a newly defined measure  $f_{eq}$ .  $f_{eq}$  is a fracture mechanics parameter, derived on the basis of  $G_F$ . The conceptual illustration of  $f_{eq}$  is shown in Fig. 9. First, consider the tension softening curve for concrete; that is, the tensile stress ( $\sigma$ ) – crack opening displacement ( $W$ ) relation. Then,  $W$  is replaced with the strain ( $\varepsilon = W/h$ ), where  $h$  is a gauge length and is assumed to be  $h=100\text{mm}$  in

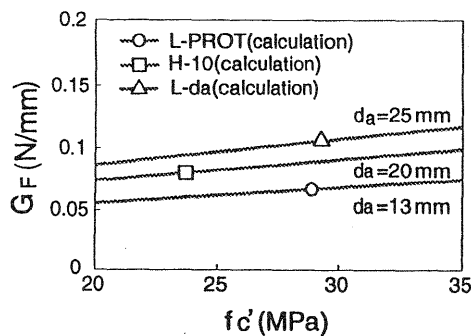


Fig.7 Variation in fracture energy

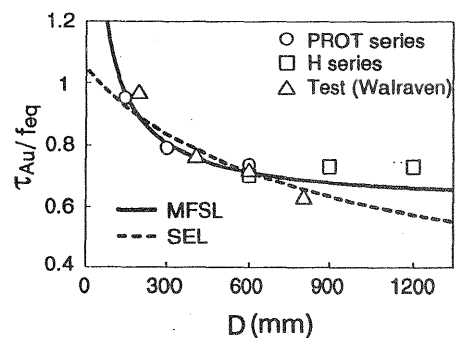


Fig.8  $\tau_{AU} / f_{eq} - D$  relation

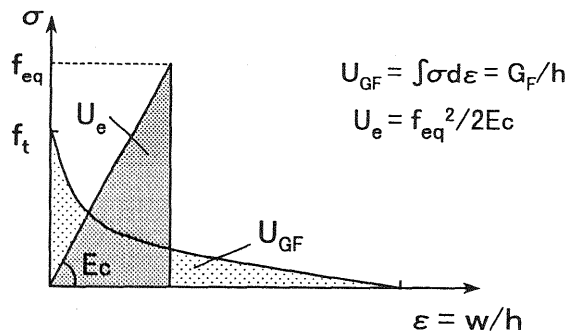


Fig.9 Concept of equivalent strength

this study. Furthermore, the area under the  $\sigma - \varepsilon$  curve; that is, the strain energy  $U_{GF}$  ( $= \int \sigma d\varepsilon$ ), is evaluated. Now, assume that concrete is the elastic body with Young's modulus of  $E_c$  subjected to an uniaxial tensile stress  $\sigma$ . Then, the strain energy of this elastic body can be defined as  $U_e = \sigma^2 / (2E_c)$ . If  $U_e = U_{GF}$  holds when  $\sigma$  reaches  $f_{eq}$ ; that is,  $\sigma = f_{eq}$ , then  $f_{eq}$  can be derived as follows:

$$f_{eq} = \sqrt{2E_c G_F / h} \quad (3)$$

In derivation of Eq. (3), the quarter-point bilinear  $\sigma - W$  relation was assumed, and we refer to  $f_{eq}$  as the "equivalent strength". In this study,  $G_F$  was calculated according to the CEB-FIP MODEL CODE 1990.

### 3 Formulation of shear strength design equation and verification

The authors attempt to introduce a size effect law into the AIJ formula, AIJ (1990), as Bazant derived the shear strength prediction formula, Bazant et al. (1987), for R/C beams by introducing it into the ACI formula, ACI (1983). The reasons why the AIJ formula is selected are first to sustain continuity and practicality of the current design formula and is secondly due to the fact that the AIJ formula is basically a rational theoretical formula derived on the basis of the lower bound theorem of plastic analysis. The AIJ formula gives the shear strength ( $Q_u$ ) as the sum of contributions from the truss mechanism ( $Q_t$ ) and the arch mechanism ( $Q_a$ ) and is expressed as follows:



$$Q_u = Q_t + Q_a = bj_t p_w \sigma_{wy} \cot \phi + \tan \theta (1 - \beta) b D v_0 \sigma_B / 2 \quad (4-1)$$

$$\text{in which, } \tan \theta = \sqrt{(L/D)^2 + 1} - L/D \quad (4-2)$$

$$\beta = \{(1 + \cot^2 \phi) p_w \sigma_{wy}\} / v_0 \sigma_B \quad (4-3)$$

$$v_0 = 0.7 - \sigma_B / 2000 \quad (4-4)$$

where,  $\sigma_B (= f'_c)$  is the compressive strength of concrete (kgf/cm<sup>2</sup>),  $p_w (= p_s)$  the shear reinforcement ratio,  $\sigma_{wy} (= f_{sy})$  the yield strength of shear reinforcement (kgf/cm<sup>2</sup>). For  $\sigma_{wy} > 25\sigma_B$ ,  $\sigma_{wy} = 25\sigma_B$ .

For  $p_w \sigma_{wy} > v_0 \sigma_B / 2$ ,  $p_w \sigma_{wy} = v_0 \sigma_B / 2$ .  $j_t$  and  $L (= a)$  are the distance between the centers of longitudinal bars in the tension and compression sides and the shear span length, respectively.  $v_0$  is the effectiveness factor of compressive strength of concrete, and  $\phi$  is the angle of compressive concrete strut in the truss mechanism and is defined as  $\cot \phi = \text{Min.} \{2.0, j_t / (D \tan \theta), \sqrt{v_0 \sigma_B / (p_w \sigma_{wy})} - 1.0\}$ . It seems that the second term in Eq. (4-1); that is,  $Q_a$ , is less reliable since  $v_0$  is an empirical parameter. On the other hand,  $Q_t$  may be predicted with a sufficient accuracy by the first term in Eq. (4-1) if stress induced in shear reinforcement is known. Here,  $Q_t$  shall be evaluated by substituting steel stress  $\sigma_s$  calculated from the observed steel strain into  $\sigma_{wy}$  in the first term of Eq. (4-1). Then, the difference between the observed  $Q_u$  and the predicted  $Q_t$  shall be defined as  $Q_a$ . Figures 10(a) and 10(b) show the variations in the truss contribution ( $\tau_t / f_{eq}$ ) and the arch contribution ( $\tau_a / f_{eq}$ ) with the increase in  $D$  value. No size effect is observed in the truss mechanism. Thus, the size effect is mainly caused by the arch mechanism. It is interesting to note that MFSL can be applicable to

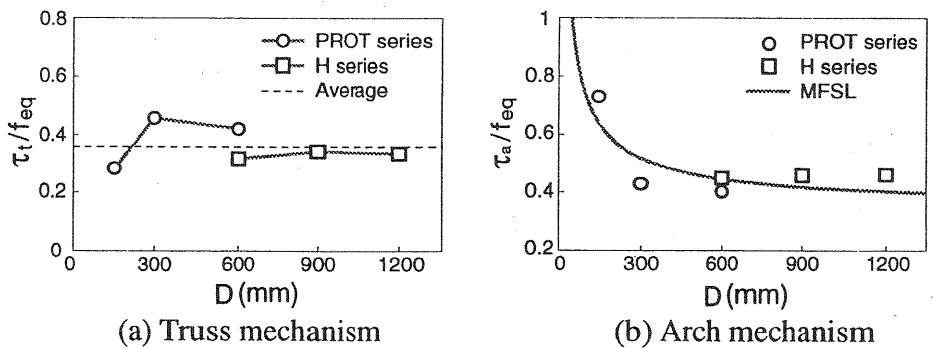


Fig.10  $\tau_t / f_{eq}$  and  $\tau_a / f_{eq}$  versus  $D$  relations

describe the size effect in the arch mechanism.

The AIJ formula assumes that the failure criterion is satisfied when resulting stress induced in the compressive concrete strut as the superposition of the truss and arch mechanisms reaches  $v_0\sigma_B$ . In the present study, the nominal strength defined by MFSL shall be applied to this criterion; that is, the failure criterion is satisfied when  $v_0\sigma_B = \sigma_N$ . Thus, after replacing  $f_t$  in Eq. (1) with  $f_{eq}$  in Eq. (3),  $\sigma_N$  can be redefined as follows:

$$\sigma_N = Bf_{eq}(1.0 + d_0/d)^{0.5} = Bf_{eq}(1.0 + \gamma d_a/d)^{0.5} \quad (5)$$

where,  $B$  and  $\gamma$  are the empirical constants and are identified as  $B=4.2$  and  $\gamma=15.0$ . Consequently, formulation of the shear strength design equation for R/C beams is completed after substituting  $\sigma_N$  in Eq. (5) into  $v_0\sigma_B$  in Eq. (4).

Figure 11(a) compares the predicted values with the test results by the authors, and Figure 11(b) compares the predicted values with the test results by Walraven et al. Note that the predicted values by the AIJ formula and the Bazant's formula are also plotted. The AIJ formula gives conservative predictions as a design formula, although poor agreement is observed. The Bazant's formula estimates the size effect fairly well, but agreement with the test results by Walraven is not sufficient. The proposed formula gives good predictions for both test results.

Finally, validity of the proposed formula is verified through the comparison with the test results on 206 R/C beam specimens failing in shear, which were collected from the works published during the past three years from 1989 to 1991. The data collected are as follows:  $D =$

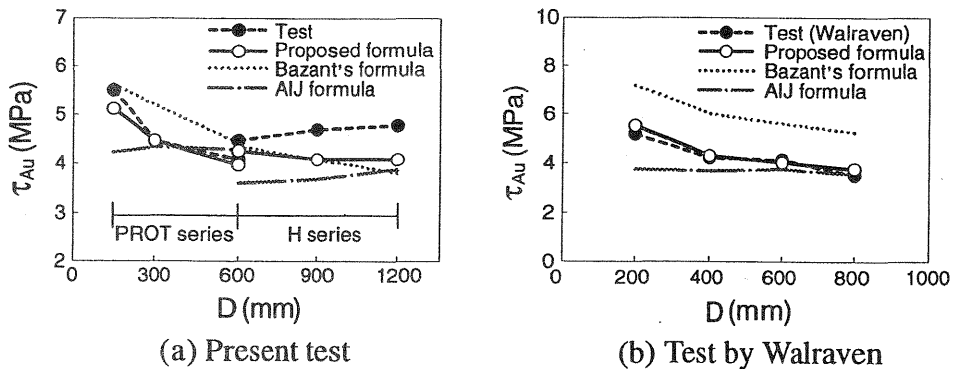


Fig.11 Nominal shear strength versus beam depth relations

100~1200mm,  $f'_c=13.8\sim119.6\text{MPa}$ ,  $p_s=0.081\sim1.76\%$ ,  $d_a=10\sim25\text{mm}$ ,  $f_{sy}=285\sim1,069\text{MPa}$ . Among these database, information on  $d_a$  was lacking in 132 out of 206 specimens. Therefore,  $d_a$  was estimated from the relation between  $D$  and  $d_a$  for the specimens that  $d_a$  is known ; that is,  $d_a=0.0486D$  for  $D < 350\text{mm}$  and  $d_a=17\text{mm}$  for  $D \geq 350\text{mm}$ . Figures 12(a), (b), (c) and (d) show the plots of ratio of the test values to the predicted values against  $D$  for the ACI formula, the AIJ formula, the Bazant's formula and the proposed formula, respectively. The ACI formula underestimates the shear strength and big scatter (Standard deviation (S.D.)=0.36) is observed. Both AIJ and Bazant's formulae give the good average values (Ave.=0.99 and 1.01), but scatter is rather significant. The proposed formula gives a little bit smaller average value and this may be due to the fact that  $d_a$  was not known in many specimens. However, it gives good agreement with the test results since scatter is much less than those of the AIJ and Bazant's formulae.

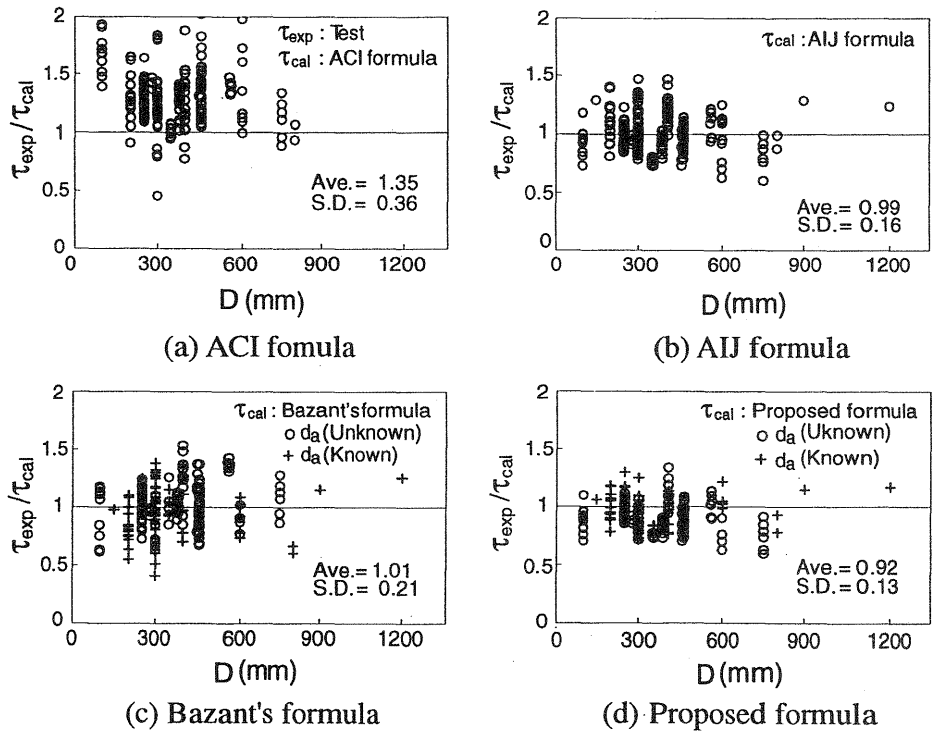


Fig.12 Comparison between predicted and test results

## 4 Conclusions

The following conclusions can be drawn through this investigation:

1. The size effect on shear strength is caused even in the R/C beams with shear reinforcement, but it tends to disappear in the range of beam depth exceeding 600~800mm.
2. The proposed equivalent strength, which is based on the fracture energy of concrete, is an effective fracture mechanics parameter to evaluate the size effect.
3. The size effect on shear strength is mainly caused in the arch mechanism, and thus a rational design formula considering the size effect can be formulated by introducing MFSL modified with the equivalent strength into the shear contribution from the arch mechanism in the AIJ formula.

**Acknowledgement** : This research was partially supported by the Ministry of Education, Science, Sports and Culture, Grant-in-Aid for Scientific Research(B), 08455265, 1997.

## 5 References

- ACI Committee 318 (1983) **Building code requirement for reinforced concrete and commentary**, American Concrete Institute.
- Architectural Institute of Japan (1990) **Design guidelines for earthquake resistant reinforced concrete buildings based on ultimate strength concept**, Maruzen, Tokyo.
- Bazant, Z.P. (1984) Size effect in blunt fracture concrete, rock, metal, **Journal of Engineering Mechanics**, 110, 518-535.
- Bazant, Z.P. and Sun, H.H. (1987) Size effect in diagonal shear failure: influence of aggregate size and stirrups, **ACI Materials Journal**, July-August, 259-272.
- Carpinteri, A., Ferro, G. and Invernizzi, S. (1995) A truncated statistical model for analyzing the size-effect on tensile strength of concrete structures, in **FRAMCOS-2** (edit. F.H. Wittmann), Vol.1, No. 6, July, 557-570.
- Comite Euro-International du Beton (CEB) (1991) **CEB-FIP MODEL CODE 1990**, Final Draft, Chapters 1-3, July, 2.5-2.6.
- Walraven, J.C. and Lehwalter, N. (1994) Size effect in short beams loaded in shear, **ACI Structural Journal**, September-October, 585-593.